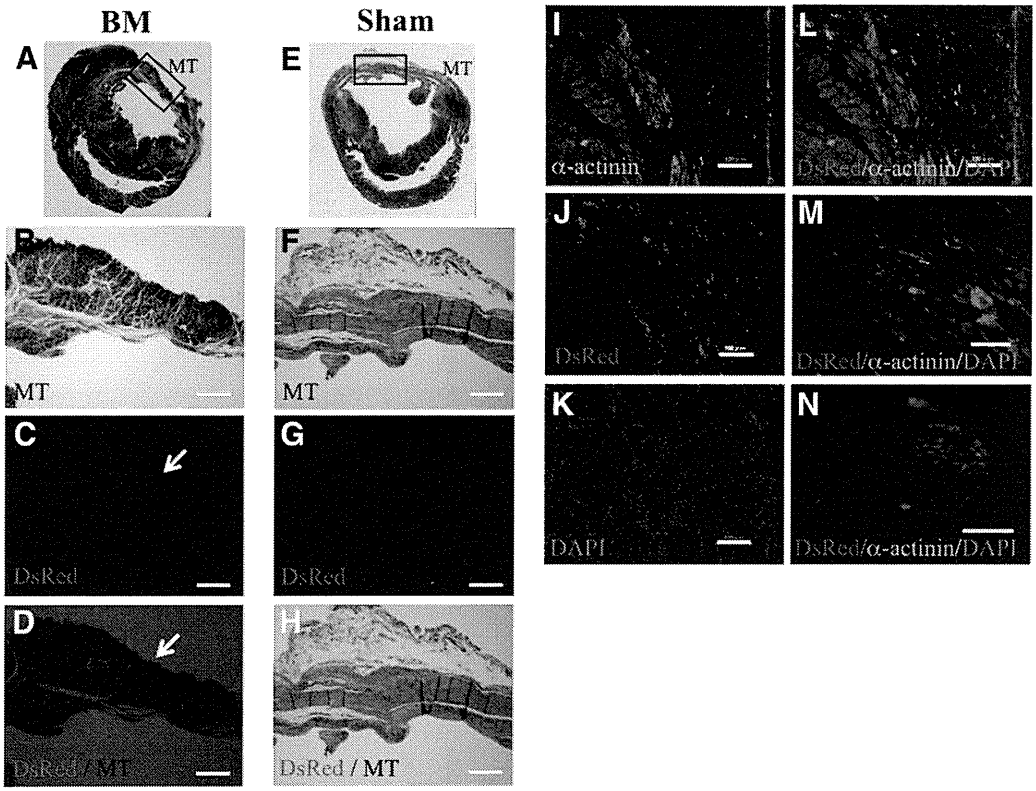

Figure 5. Histological examination of short-axis specimens at 4 weeks. **(A–H):** Microscopic images showing the whole heart and the anterior wall region in the BM group **(A–D)** and the sham group **(E–H)**. MT staining **(A, B, E, F)**. DsRed **(C, G)** was expressed in the cytosol of induced pluripotent stem (iPS) cell-derived cells in the BM group. **(D):** Merged image of **(B)** and **(C)**. **(H):** Merged image of **(F)** and **(G)**. The iPS cell-derived BM survived at the epicardial implantation site (arrows in **[C, D]**), attenuated fibrosis, and increased the thickness of the anterior wall. Scale bars = 500 μm. **(I–N):** Fluorescent microscopic images showing a part of the anterior wall region in the BM group. **(I):** Immunofluorescent histochemistry of α-actinin. DsRed was expressed in the cytosol of iPS-derived cells **(J)**; the nuclei were stained with DAPI **(K)**. **(L):** Merged image of **(I–K)**. Scale bars = 100 μm. **(M, N):** High-magnification images showing the colocalization of surviving DsRed- and α-actinin-positive cells in the anterior wall. Scale bars = 40 **(K)** and 10 μm **(L)**. Abbreviations: BM, bioengineered myocardium; DAPI, 4′,6-diamidino-2-phenylindole; DsRed, *Discosoma* red fluorescent protein; MT, Masson's trichrome.

not use a dissociation solution such as StemPro Accutase (Life Technologies, Carlsbad, CA, http://www.lifetechnologies.com) or trypsin. Therefore, α-actinin$^+$ cells were not arranged uniformly in the BM sheet, and its thickness varied throughout. For example, the section of EBs were thicker than the region of outgrowth of cells from EBs, and there were some small holes in the BM, likely representing areas of dead cells resulting from the use of no-glucose DMEM. Host cells are more likely to migrate into such areas. ELISA results revealed that elevated levels of HGF and VEGF probably contributed to the improvement of systolic performance by inducing angiogenesis and the migration of some stem cells, as observed with the implantation of skeletal myoblast sheets. Alternatively, the nondamaged host myocardium probably continues to survive after LAD coronary ligation because of the multiple autocrine or paracrine effects induced by the implanted BM, thereby improving the systolic and diastolic performances.

iPS cells can cause tumors such as teratomas; therefore, there is some apprehension regarding their use in clinical settings. We did not observe SSEA-1-positive cells by immunostaining analysis in the no-glucose DMEM-treated group. However, it is also important to acknowledge that it takes only one cell to form a tumor, and it is virtually impossible to guarantee that 100% of the cells are differentiated and safe. Therefore, to investigate the effect of no-glucose DMEM treatment on cardiomyocyte purification, we examined mice for teratomas after implantation of the BM that had been maintained for various times in no-glucose DMEM. The teratoma formation (TF) rate decreased as the period of no-glucose DMEM treatment was extended, and there was no TF in the 3-day no-glucose DMEM treatment group (supplemental online Fig. 5). Therefore, any undifferentiated cells cannot survive in no-glucose DMEM for more than 3 days.

Conclusion

We propose that the BM derived from iPS cells can improve cardiac performance and attenuate remodeling in a rat infarction model. Additional studies are required to confirm the mechanical and electrical functions in vivo; nevertheless, the BM derived from iPS cells may be a promising part of the armamentarium for the treatment of heart failure.

Acknowledgments

We thank Masako Yokoyama and Yuka Fujiwara for their excellent technical assistance. This study was partially supported by

the Japan Science and Technology Agency. K.M. is a research fellow at the Japan Society for the Promotion of Science.

Author Contributions

K.M.: conception and design, data collection, data interpretation, manuscript writing; H.U.: conception and design, data collection, data interpretation, manuscript writing assistance; A.S.: conception and design, data interpretation, manuscript revision, final approval; S.M.: conception and design, data interpretation, manuscript writing and revision, final approval; T. Sakaguchi: data interpretation; T.H.: data collection, data interpretation; T. Shimizu and T.O.: methodological assistance; S.Y.: conception and design, methodological help; Y.S.: conception and design, administrative and financial support, data interpretation, final approval.

Disclosure of Potential Conflicts of Interest

The authors indicate no potential conflicts of interest.

References

1 Lloyd-Jones D, Adams RJ, Brown TM et al. Heart disease, stroke statistics—2010 update: A report from the American Heart Association. Circulation 2010;121:e46–e215.

2 Towbin JA, Bowles NE. The failing heart. Nature 2002;415:227–233.

3 Dimmeler S, Zeiher AM, Schneider MD. Unchain my heart: The scientific foundations of cardiac repair. J Clin Invest 2005;115:572–583.

4 Murry CE, Field LJ, Menasché P. Cell-based cardiac repair: Reflections at the 10-year point. Circulation 2005;112:3174–3183.

5 Segers VF, Lee RT. Stem-cell therapy for cardiac disease. Nature 2008;451:937–942.

6 Bolli R, Chugh AR, D'Amario D et al. Cardiac stem cells in patients with ischaemic cardiomyopathy (SCIPIO): Initial results of a randomised phase 1 trial. Lancet 2011;378:1847–1857.

7 Gnecchi M, He H, Liang OD et al. Paracrine action accounts for marked protection of ischemic heart by Akt-modified mesenchymal stem cells. Nat Med 2005;11:367–368.

8 Ebelt H, Jungblut M, Zhang Y et al. Cellular cardiomyoplasty: Improvement of left ventricular function correlates with the release of cardioactive cytokines. Stem Cells 2007;25:236–244.

9 Shintani Y, Fukushima S, Varela-Carver A et al. Donor cell-type specific paracrine effects of cell transplantation for post-infarction heart failure. J Mol Cell Cardiol 2009;47:288–295.

10 Uemura R, Xu M, Ahmad N et al. Bone marrow stem cells prevent left ventricular remodeling of ischemic heart through paracrine signaling. Circ Res 2006;98:1414–1421.

11 Li X, Yu X, Lin Q et al. Bone marrow mesenchymal stem cells differentiate into functional cardiac phenotypes by cardiac microenvironment. J Mol Cell Cardiol 2007;42:295–303.

12 Reinecke H, Minami E, Zhu WZ et al. Cardiogenic differentiation, transdifferentiation of progenitor cells. Circ Res 2008;103:1058–1071.

13 Jackson KA, Majka SM, Wang H et al. Regeneration of ischemic cardiac muscle, vascular endothelium by adult stem cells. J Clin Invest 2001;107:1395–1402.

14 Nygren JM, Jovinge S, Breitbach M et al. Bone marrow-derived hematopoietic cells generate cardiomyocytes at a low frequency through cell fusion, but not transdifferentiation. Nat Med 2004;10:494–501.

15 Okano T, Yamada N, Sakai H et al. A novel recovery system for cultured cells using plasma-treated polystyrene dishes grafted with poly(*N*-isopropylacrylamide). J Biomed Mater Res 1993;27:1243–1251.

16 Shimizu T, Yamato M, Isoi Y et al. Fabrication of pulsatile cardiac tissue grafts using a novel 3-dimensional cell sheet manipulation technique, temperature-responsive cell culture surfaces. Circ Res 2002;90:e40–e48.

17 Shimizu T, Yamato M, Kikuchi A et al. Cell sheet engineering for myocardial tissue reconstruction. Biomaterials 2003;24:2309–2316.

18 Pagani FD, DerSimonian H, Zawadzka A et al. Autologous skeletal myoblasts transplanted to ischemia-damaged myocardium in humans. Histological analysis of cell survival, differentiation. J Am Coll Cardiol 2003;41:879–888.

19 Suzuki K, Murtuza B, Fukushima S et al. Targeted cell delivery into infarcted rat hearts by retrograde intracoronary infusion: Distribution, dynamics, and influence on cardiac function. Circulation 2004;110(suppl 1):II225–II230.

20 Menasché P, Hagege AA, Vilquin JT et al. Autologous skeletal myoblast transplantation for severe postinfarction left ventricular dysfunction. J Am Coll Cardiol 2003;41:1078–1083.

21 Memon IA, Sawa Y, Fukushima N et al. Repair of impaired myocardium by means of implantation of engineered autologous myoblast sheets. J Thorac Cardiovasc Surg 2005;130:1333–1341.

22 Takahashi K, Yamanaka S. Induction of pluripotent stem cells from mouse embryonic, adult fibroblast cultures by defined factors. Cell 2006;126:663–676.

23 Takahashi K, Tanabe K, Ohnuki M et al. Induction of pluripotent stem cells from adult human fibroblasts by defined factors. Cell 2007;131:861–872.

24 Yu J, Vodyanik MA, Smuga-Otto K et al. Induced pluripotent stem cell lines derived from human somatic cells. Science 2007;318:1917–1920.

25 Zhang J, Wilson GF, Soerens AG et al. Functional cardiomyocytes derived from human induced pluripotent stem cells. Circ Res 2009;104:e30–e41.

26 Zwi L, Caspi O, Arbel G et al. Cardiomyocyte differentiation of human induced pluripotent stem cells. Circulation 2009;120:1513–1523.

27 Yokoo N, Baba S, Kaichi S et al. The effects of cardioactive drugs on cardiomyocytes derived from human induced pluripotent stem cells. Biochem Biophys Res Commun 2009;387:482–488.

28 Nakagawa M, Koyanagi M, Tanabe K et al. Generation of induced pluripotent stem cells without Myc from mouse, human fibroblasts. Nat Biotechnol 2008;26:101–106.

29 Naito AT, Shiojima I, Akazawa H et al. Developmental stage-specific biphasic roles of Wnt/beta-catenin signaling in cardiomyogenesis, hematopoiesis. Proc Natl Acad Sci USA 2006;103:19812–19817.

30 Miyagawa S, Sawa Y, Sakakida S et al. Tissue cardiomyoplasty using bioengineered contractile cardiomyocyte sheets to repair damaged myocardium: Their integration with recipient myocardium. Transplantation 2005;80:1586–1595.

31 Sekiya N, Matsumiya G, Miyagawa S et al. Layered implantation of myoblast sheets attenuates adverse cardiac remodeling of the infarcted heart. Thorac J Cardiovasc Surg 2009;138:985–993.

See www.StemCellsTM.com for supporting information available online.

Bioengineered Myocardium Derived from Induced Pluripotent Stem Cells Improves Cardiac Function and Attenuates Cardiac Remodeling Following Chronic Myocardial Infarction in Rats

Kenji Miki, Hisazumi Uenaka, Atsuhiro Saito, Shigeru Miyagawa, Taichi Sakaguchi, Takahiro Higuchi, Tatsuya Shimizu, Teruo Okano, Shinya Yamanaka and Yoshiki Sawa

Stem Cells Trans Med 2012;1;430-437; originally published online May 14, 2012;
DOI: 10.5966/sctm.2011-0038

Circulation
JOURNAL OF THE AMERICAN HEART ASSOCIATION

American Heart Association®

Feasibility, Safety, and Therapeutic Efficacy of Human Induced Pluripotent Stem Cell-Derived Cardiomyocyte Sheets in a Porcine Ischemic Cardiomyopathy Model

Masashi Kawamura, Shigeru Miyagawa, Kenji Miki, Atsuhiro Saito, Satsuki Fukushima, Takahiro Higuchi, Takuji Kawamura, Toru Kuratani, Takashi Daimon, Tatsuya Shimizu, Teruo Okano and Yoshiki Sawa

Circulation. 2012;126:S29-S37
doi: 10.1161/CIRCULATIONAHA.111.084343
Circulation is published by the American Heart Association, 7272 Greenville Avenue, Dallas, TX 75231

Print ISSN: 0009-7322. Online ISSN: 1524-4539

Feasibility, Safety, and Therapeutic Efficacy of Human Induced Pluripotent Stem Cell-Derived Cardiomyocyte Sheets in a Porcine Ischemic Cardiomyopathy Model

Masashi Kawamura, MD; Shigeru Miyagawa, MD, PhD; Kenji Miki, MSc; Atsuhiro Saito, PhD; Satsuki Fukushima, MD, PhD; Takahiro Higuchi, MD; Takuji Kawamura, MD; Toru Kuratani, MD, PhD; Takashi Daimon, PhD; Tatsuya Shimizu, MD, PhD; Teruo Okano, PhD; Yoshiki Sawa, MD, PhD

Background—Human induced pluripotent stem cell-derived cardiomyocytes (hiPS-CMs) are a promising source of cells for regenerating myocardium. However, several issues, especially the large-scale preparation of hiPS-CMs and elimination of undifferentiated iPS cells, must be resolved before hiPS cells can be used clinically. The cell-sheet technique is one of the useful methods for transplanting large numbers of cells. We hypothesized that hiPS-CM-sheet transplantation would be feasible, safe, and therapeutically effective for the treatment of ischemic cardiomyopathy.

Methods and Results—Human iPS cells were established by infecting human dermal fibroblasts with a retrovirus carrying Oct3/4, Sox2, Klf4, and c-Myc. Cardiomyogenic differentiation was induced by WNT signaling molecules, yielding hiPS-CMs that were almost 90% positive for α-actinin, Nkx2.5, and cardiac troponin T. hiPS-CM sheets were created using thermoresponsive dishes and transplanted over the myocardial infarcts in a porcine model of ischemic cardiomyopathy induced by ameroid constriction of the left anterior descending coronary artery (n=6 for the iPS group receiving sheet transplantation and the sham-operated group; both groups received tacrolimus daily). Transplantation significantly improved cardiac performance and attenuated left ventricular remodeling. hiPS-CMs were detectable 8 weeks after transplantation, but very few survived long term. No teratoma formation was observed in animals that received hiPS-CM sheets.

Conclusions—The culture system used yields a large number of highly pure hiPS-CMs, and hiPS-CM sheets could improve cardiac function after ischemic cardiomyopathy. This newly developed culture system and the hiPS-CM sheets may provide a basis for the clinical use of hiPS cells in cardiac regeneration therapy. **(*Circulation*. 2012;126[suppl 1]:S29–S37.)**

Key Words: pluripotent stem cell ■ regeneration therapy ■ transplantation

The myocardium has limited regenerative capacity, and loss of myocardium due to myocardial infarction therefore leads to heart failure. Despite remarkable recent progress in medical and surgical treatments for heart failure, end-stage heart failure remains a leading cause of morbidity and mortality.[1] Therefore, the myocardium is one of the most important targets in regenerative medicine. Cell therapy has been introduced as a new treatment for heart failure. Clinical trials using bone marrow cells and myoblasts are underway; although these cells improve cardiac performance, chiefly through paracrine cytokine effects, they show limited differentiation into cardiomyocytes.[2]

Induced pluripotent stem (iPS) cells were first generated by nuclear reprogramming of mouse fibroblasts in 2006,[3] and human iPS (hiPS) cells were established in 2007 by the transduction of defined factors.[4,5] The production of hiPS cells poses fewer legal and ethical issues than does the generation of human embryonic stem (ES) cells. In addition, recent studies have demonstrated methods for the highly efficient production from hiPS cells of cardiomyocytes with typical electrophysiological function and pharmacological responsiveness.[6,7] Human iPS cells represent an unlimited source of cardiomyocytes because of their great potential for differentiation and are therefore one of the most promising sources of cells for cardiac regenerative therapy.[8,9] Nevertheless, many important problems, especially the large-scale preparation of cardiomyocytes by differentiation of iPS cells and the elimination of undifferentiated iPS cells to avoid teratoma formation, must be addressed before hiPS cells can be used clinically.[8,9]

The recently developed scaffoldless tissue engineering technique of cell-sheet engineering is applicable to myocar-

From the Department of Cardiovascular Surgery, Osaka University Graduate School of Medicine, Suita, Osaka, Japan (M.K., S.M., K.M., S.F., T.H., T. Kawamura, T. Kuratani, Y.S.); the Medical Center for Translational Research, Osaka University Hospital, Suita, Osaka, Japan (A.S.); the Department of Biostatistics, Hyogo College of Medicine, Nishinomiya, Hyogo, Japan (T.D.); and the Institute of Advanced Biomedical Engineering and Science, TWIns, Tokyo Women's, Medical University, Shinjuku-ku, Tokyo, Japan (T.S., T.O.).

Presented at the 2011 American Heart Association meeting in Orlando, FL, November 13–17, 2011.

The online-only Data Supplement is available at http://circ.ahajournals.org/lookup/suppl/doi:10.1161/CIRCULATIONAHA.111.084343/-/DC1.

Correspondence to Yoshiki Sawa, MD, PhD, 2-2 Yamada-oka, Suita, Osaka, 565-0871, Japan. E-mail sawa-p@surg1.med.osaka-u.ac.jp

Circulation **is available at http://circ.ahajournals.org** **DOI: 10.1161/CIRCULATIONAHA.111.084343**

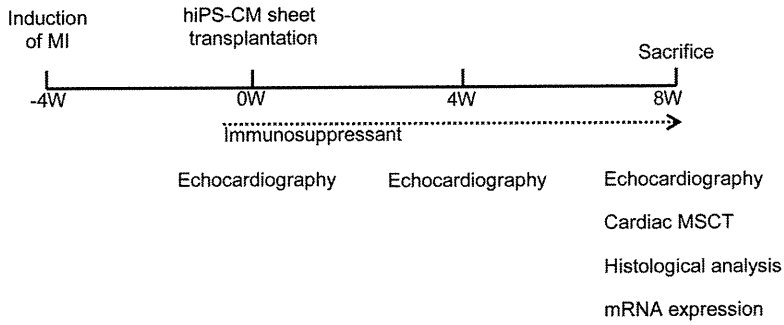

Figure 1. Study protocol of the minipig experiment and the evaluation of cardiac function and histological analysis.

dial regeneration therapy.[10] In contrast to the needle injection technique, the cell-sheet technique can deliver a large number of cells to damaged myocardium without the loss of transplanted cells or injury to the host myocardium. We have previously reported that use of the cell-sheet technique with autologous skeletal myoblasts improves cardiac function in small and large animal models of ischemic cardiomyopathy.[11,12]

We hypothesized that hiPS-derived cardiomyocyte (hiPS-CM)-sheet transplantation would be therapeutically effective in the context of ischemic cardiomyopathy. In this study, we examined the following aspects of this procedure: stable in vitro culture of a large number of cardiomyocytes by differentiation of hiPS cells, generation of hiPS-CM sheets for clinical applications using temperature-responsive dishes, survival of hiPS-CM sheets in the myocardium of a large animal, and the direct contribution of these sheets to the improvement of cardiac performance by structural and electromechanical integration into the recipient myocardium, without teratoma formation, in a porcine ischemic cardiomyopathy model.

Materials and Methods

Animal care complied with the "Guide for the Care and Use of Laboratory Animals" (National Institutes of Health publication No. 85-23, revised 1996). Experimental protocols were approved by the Ethics Review Committee for Animal Experimentation of Osaka University Graduate School of Medicine.

Culture, Differentiation, and Purification of hiPS Cells and Collection of Conditioned Medium

The hiPS cell line 201B7 that was generated using the 4 transcription factors Oct4, Sox2, Klf4, and c-Myc (a generous gift from Professor Yamanaka, Kyoto University, Kyoto, Japan) was used in this study.[4] The hiPS cells were cultured on Matrigel (BD Bioscience)-coated dishes in mTeSR1 medium (Stem Cell Technologies).

Human iPS cells were then dissociated using StemPro Accutase Cell Dissociation Reagent (Invitrogen), transferred to Corning ultralow-attachment surface culture dishes (Sigma-Aldrich) at a density of 50 000 cells/mL in mTeSR1 with Y-27632 (Wako), and cultured for 4 days to allow them to form embryoid bodies. The embryoid bodies were replated with differentiation medium (DMEM-F12; Invitrogen) containing 20% fetal bovine serum, 100 μmol/L nonessential amino acids (Invitrogen), 50 U/mL penicillin, 50 mg/mL streptomycin (Invitrogen), and 5.5 mmol/L 2-mercaptoethanol (Invitrogen) and supplemented with 100 ng/mL Wnt3a (R&D Systems) and 100 ng/mL R-Spondin-1 (Stem RD) and cultured for 2 days. The culture medium was then replaced with differentiation medium without the supplemental factors for 2 days and then changed to differentiation medium supplemented with 100 ng/mL Dkk1 (R&D Systems) for 2 days. On Day 10, the embryoid bodies were plated on gelatin-coated dishes in differentiation medium, which was refreshed every 2 days.

The culture medium was subsequently replaced with no-glucose Dulbecco modified Eagle medium (Invitrogen) with 1 mmol/L lactic acid (Wako; F. Hattori and K. Fukuda. WO2007/088874; PCT/JP2007/051563, 2007) on Day 20 and changed to Dulbecco modified Eagle medium/10% fetal bovine serum the next day. On Day 25, the culture medium was again replaced with no-glucose Dulbecco modified Eagle medium with 1 mmol/L lactic acid and changed to Dulbecco modified Eagle medium/10% fetal bovine serum the next day; this procedure eventually generated pure hiPS-CM. The hiPS-CMs were then labeled with a red fluorescent marker (CellTracker Red CMTPX; Invitrogen) as previously described.[13]

Fetal bovine serum-free Dulbecco modified Eagle medium media were conditioned by hiPS-CMs for 48 hours after the completion of our differentiation and purification protocols. A total of 48 cytokines and growth factors were measured by the Bio-Plex human cytokine assay (Bio-Rad) for in vitro screening.

Preparation of hiPS Cell-Derived Cardiomyocyte Sheets

The hiPS-CMs were detached using StemPro Accutase Cell Dissociation Reagent and seeded onto 6-cm UpCell dishes (CellSeed). The next day, the dish was incubated at room temperature, which caused the cells to detach spontaneously to form scaffold-free hiPS-CM sheets.

Generation of the Porcine Chronic Myocardial Infarction Model and hiPS-CM Sheet Transplantation

A chronic myocardial infarction model was generated by placement of an ameroid constrictor (COR-2.50-SS; Research Instruments) around the left anterior descending coronary artery in female minipigs (Japan Farm) weighing 20 to 25 kg[14] (Figure 1). Four weeks after myocardial infarction induction, transplantation of hiPS-CM sheets was performed through median sternotomy under general anesthesia. All animals were immunosuppressed with daily intake of tacrolimus (0.6 mg/kg; Astellas) from 5 days before transplantation until euthanasia. The minipigs were randomly divided into 2 treatment groups, either hiPS-CM sheet transplantation (iPS group) or sham operation (n=6 each).

Standard and 2-Dimensional Speckle-Tracking Echocardiography

Transthoracic echocardiography was performed under general anesthesia using a 5.0-MHz transducer (Aplio Artida). The left ventricular (LV) end-diastolic and end-systolic diameters were measured, whereas the LV end-diastolic and end-systolic volumes (LVEDV and LVESV, respectively) were calculated from the Teichholz formula.[15] The LV ejection fraction (LVEF) was calculated from the following formula: LVEF (%)=100×(LVEDV−LVESV)/(LVEDV).

Two-dimensional speckle-tracking echocardiography analysis was performed using the customized 2-dimensional speckle-tracking echocardiography software for the Toshiba system (2D Wall Motion Tracking). Regional cardiac function was evaluated using radial strain values obtained from the midshort-axis plane and expressed as a percentage.

Cardiac CT Scan

Electrocardiography-gated multislice CT was performed in the supine position with a 16-slice multislice CT scanner (Somatron Emotion 16; Siemens) during end-expiratory breathhold under general anesthesia. Multislice CT was performed after intravenous injection of 90 mL of nonionic contrast medium (Iomeprol; Bracco Imaging). Axial images were reconstructed using the scanner software. All images were analyzed on a workstation (AZE; Virtual Pl Lexus 64). LVEDV and LVESV were obtained from the workstation and LVEF was calculated using the formula described previously.

Holter Electrocardiography

Holter electrocardiography was performed for 24 hours in both groups (n=6 each). The arrhythmogenesis associated with hiPS-CM sheet transplantation was evaluated based on the number of premature ventricular contractions.

Histology, Immunohistolabeling, and Fluorescence In Situ Hybridization

Dissociated cultured cells were fixed in 4% paraformaldehyde. Primary antibodies included anticardiac troponin T (cTNT; Abcam), anti-Nkx2.5 (Santa Cruz Biotechnology), anti-α-actinin (Sigma-Aldrich), antihuman CD31 (BD Bioscience), antihuman CD34 (BD Bioscience) and antivimentin (BD Bioscience) visualized by fluorescent-conjugated secondary antibodies such as AlexaFluor488 goat antirabbit IgG, AlexaFluor488 goat antimouse IgG, and AlexaFluor488 donkey antigoat IgG (Invitrogen) with counterstaining by 4′6-diamidino-2-phenylindole (Dojindo) and assessed by fluorescence microscopy. Images of the samples were acquired with a Biorevo BZ-9000 (Keyence). Positivity of the cardiomyocyte-specific markers or other lineage markers in the cultured cells was determined from the acquired images by using computer-based cell counting with the Dynamic Cell Count BZ-H1CE software (Keyence).

The excised heart specimen was fixed with either 10% buffered formalin or 4% paraformaldehyde for frozen sections. Picrosirius red or periodic acid-Schiff stains were used to assess interstitial fibrosis or cardiomyocyte hypertrophy, respectively. To evaluate neovascularization in the peri-infarct area, immunolabeling with antihuman von Willebrand factor antibody (Dako) was done. The frozen sections were immunolabeled by the primary antibodies such as anticTNT (Abcam) and antislow myosin heavy chain (Sigma-Aldrich) antibodies, visualized by AlexaFluor488 goat antimouse IgG (Invitrogen), counterstained by 4′,6-diamidino-2-phenylindole, and assessed by fluorescence microscopy or confocal laser microscopy.

The hiPS-CMs at 8 weeks after transplantation were detected by fluorescent in situ hybridization using a human specific genomic probe labeled by Cy3 (Chromosome Science Labs). The samples were double-stained with other antibodies described previously and counterstained with 4′,6-diamidino-2-phenylindole.

Real-Time Polymerase Chain Reaction

Total RNA was extracted from cardiac tissue and reverse transcribed using TaqMan reverse transcription reagents (Applied Biosystems), and real-time polymerase chain reaction was performed with the ABI PRISM 7700 (Applied Biosystems) system using pig-specific primers for vascular endothelial growth factor and basic fibroblast growth factor. The average copy number of gene transcripts was normalized to that of glyceraldehyde-3-phosphate dehydrogenase for each sample.

Statistical Analysis

JMP software (JMP7.01; SAS Institute Inc) was used for all statistical analyses. Continuous values are expressed as the mean±SD. Within-group differences were compared with the Wilcoxon signed-rank test and between-group differences with the Wilcoxon-Mann-Whitney U test because the sample sizes are too small (just n=6 in each group and n=6 pairs) to allow checking of the assumptions of the unpaired and paired t tests, respectively. A probability value <0.05 was considered statistically significant.

Results

Generation of Highly Purified hiPS-CM Sheets

Cardiomyogenic differentiation of hiPS cells was induced by treatment of the embryoid bodies formed from cultured hiPS cells with Wnt3a and R-Spondin-1. Subsequently, the differentiated hiPS cells were purified by culture in glucose-free medium to yield hiPS-CMs. The hiPS-CMs were highly positive for the cardiomyocyte-specific markers α-actinin (89.7%±3.8%), cTNT (87.4%±4.2%), and Nkx2.5 (84.2%± 4.3%), as assessed by immunohistolabeling (Figure 2A–D). In addition, the hiPS-CMs included a small population of cells expressing vascular endothelial or endothelial progenitor cell-specific markers such as CD31 (2.9%±3.0%) and CD34 (1.6%±1.4%; Figures 2A, 2E, and 2F). These cells also included a small population of vimentin-positive cells (2.4%±1.0%), which is a marker of fibroblast or smooth muscle cells (Figures 2A and 2G).

Serum-free conditioned media from hiPS-CMs were screened for the secreted factors by using enzyme-linked immunosorbent assay (Figure 2H–I). The media contained high concentrations of various factors such as hepatocyte growth factor (HGF), stromal cell-derived factor (SDF), interluekin 6, leukemia inhibitory factor (LIF), macrophage migration inhibitory factor (MIF), and monocyte chemoattractant protein-1.

Subsequently, culture in the thermoresponsive dishes yielded round-shaped scaffold-free hiPS-CM sheets (Figure 2J). Hematoxylin & eosin-stained cross-sections of the sheet showed a 30- to 50-μm-thick regular structure with abundant extracellular matrix (Figure 2K). Immunohistolabeling showed that the cytoplasm of most of the cells in the hiPS-CM sheets was homogeneously positive for cTNT (Figure 2L).

Feasibility and Safety of hiPS-CM Sheet Transplantation Into the Chronic Myocardial Infarction Heart

Transplantation of 8 hiPS-CM sheets was successfully performed through median sternotomy under general anesthesia in 6 immunosuppressed minipigs with LVEF values of 35% to 45% due to induced chronic myocardial infarction. There was no mortality related to the procedure or otherwise before the planned euthanasia. Twenty-four-hour electrocardiography monitoring only rarely identified ventricular arrhythmias in either group before the planned euthanasia (data not shown). In addition, no teratomas were formed in the heart or other thoracic organs within the 8 weeks after the transplantation of the hiPS-CM sheets (data not shown).

Global Cardiac Functional Recovery After hiPS-CM-Sheet Transplantation

Serial standard transthoracic echocardiography was performed before and 4 and 8 weeks after the cell-sheet transplantation or sham surgery. The baseline LV end-diastolic diameter, LV end-systolic diameter, and LVEF did not differ significantly between the 2 groups. The sham-operated pigs showed nonsignificant upward trends in LV end-diastolic diameter and LV end-systolic diameter and a downward trend in LVEF between 4 and 8 weeks after surgery (Figure 3A–C). LVEF was significantly greater in the iPS group than in the sham group after 4 (53.2%±4.3% versus 38.3%±4.3%, $P<0.01$) and 8 (51.6%±4.9% versus 36.0%±5.9%, $P<0.01$) weeks. LV

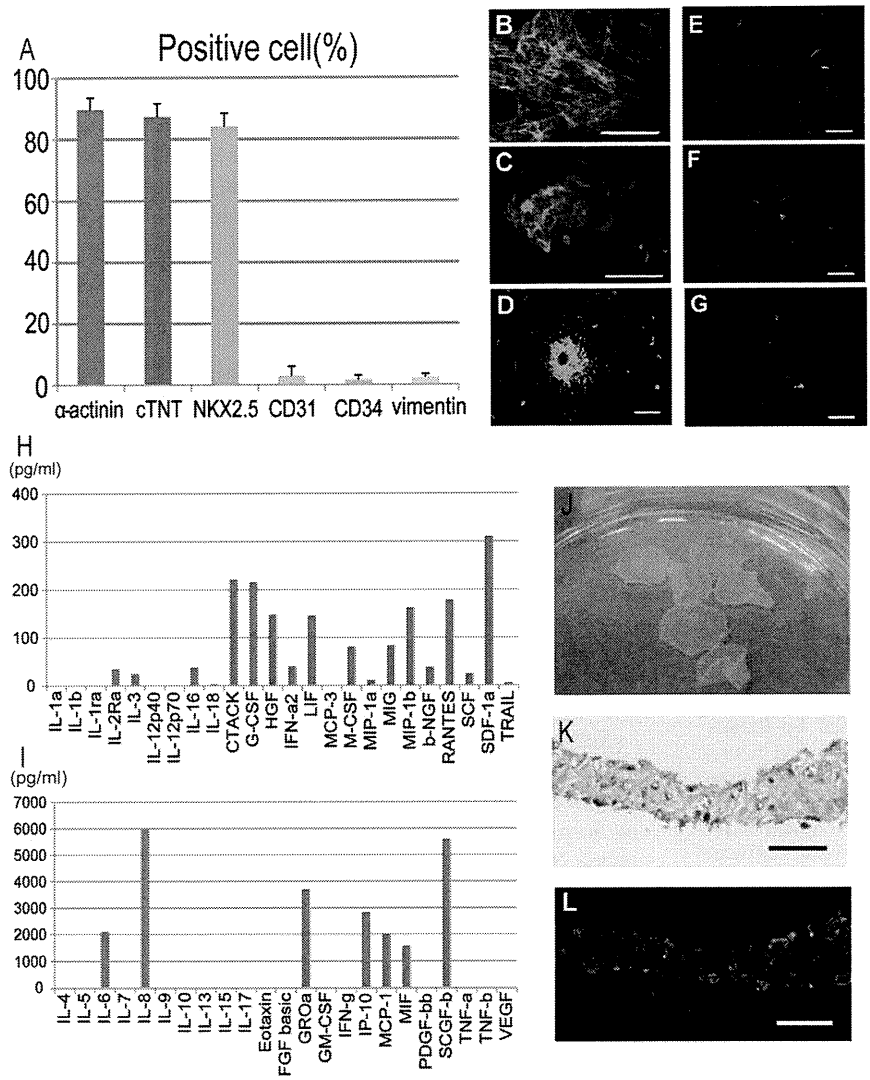

Figure 2. Histological characteristics of the hiPS-CM sheets. **A**, quantitative analysis of the numbers of hiPS-derived cells expressing α-actinin, cTNT, Nkx2.5, CD31, CD34, or vimentin, shown as percentages (%). Almost 90% pure cardiomyocytes were obtained. **B–G**, Immunostaining of the hiPS-CMs with anti-α-actinin (**B**), anticTNT (**C**), and anti-Nkx2.5 (**D**), anti-CD31 (**E**), anti-CD34 (**F**), and antivimentin (**G**) antibodies in green; bar=100 μm in **B–G. H–I**, In vitro screening for cytokines and growth factors. Several factors that may potentially be involved in cardiac repair were detected at relatively high concentrations in the medium. **J**, hiPS-CM sheets in a 10-cm dish. **K–L**, Hematoxylin and eosin (HE) staining (**K**) and immunostaining with cTNT antibody (**L**) of the hiPS-CM sheets in green. Many cTNT-positive cells were detected in the hiPS-CM sheets; bar=50 μm in **K–L**. The cell nuclei were counterstained with 4′,6-diamidino-2-phenylindole (DAPI) in blue (**B, C, E, F, G, L**). hiPS-CM indicates human induced pluripotent stem cell-derived cardiomyocyte.

end-systolic diameter was significantly smaller in the iPS group than in the sham group after 4 (25.0±1.9 mm versus 30.1±3.4 mm, $P<0.05$) and 8 (26.2±3.3 mm versus 34.7±5.4 mm, $P<0.05$) weeks, whereas LV end-diastolic diameter did not differ significantly between the 2 groups.

A cardiac multislice CT scan was performed 8 weeks after the treatment and also demonstrated that LVEF was significantly greater in the iPS group (50.7%±5.4%) than in the sham group (40.5%±1.7%, $P<0.05$; Figure 4A). LVEDV and LVESV were significantly smaller in the iPS group than in the sham group (57.1±7.5 mL versus 76.1±4.1 mL, $P<0.05$, and 28.3±6.0 mL versus 45.3±3.0 mL, $P<0.05$, respectively; Figure 4B–C).

Recovery of Regional LV Wall Motion After hiPS-CM Sheet Transplantation

Serial speckle-tracking echocardiography was performed to compare the strain values at baseline and 4 weeks after the treatment. Radial strain was measured from the midshort-axis plane to evaluate regional wall motion (Figure 5B–C). In the sham group, the radial strain levels in the infarct, the border, and the remote area had not changed significantly after 4 weeks relative to the baseline values. In contrast, in the iPS group, the radial strain in the border area was significantly greater after 4 weeks than at baseline (10.35%±4.17% versus 15.22%±1.66%, $P<0.05$), whereas the radial strain levels in the infarct and the remote area had not changed significantly.

Pathological Hypertrophy, Interstitial Fibrosis, and Vascular Density

The pathological cardiomyocyte hypertrophy, interstitial fibrosis, and vascular density 8 weeks after the treatment were assessed semiquantitatively by periodic acid-Schiff staining, picrosirius red staining, and immunohistochemistry for von Willebrand factor, respectively (Figure 6). The diameters of the cardiomyocytes in the remote area were significantly smaller in the iPS group than in the sham group. There was consistently significantly less accumulation of interstitial fibrosis in the remote area in the iPS group than in the sham group. In addition, the vascular density in the border area was significantly greater in the iPS group than in the sham group.

Upregulation of Vascular Endothelial Growth Factor and Basic Fibroblast Growth Factor Expression in the Border Area After Treatment

The expression levels of growth factors that are expressed in the myocardium and are potentially related to neovascular-

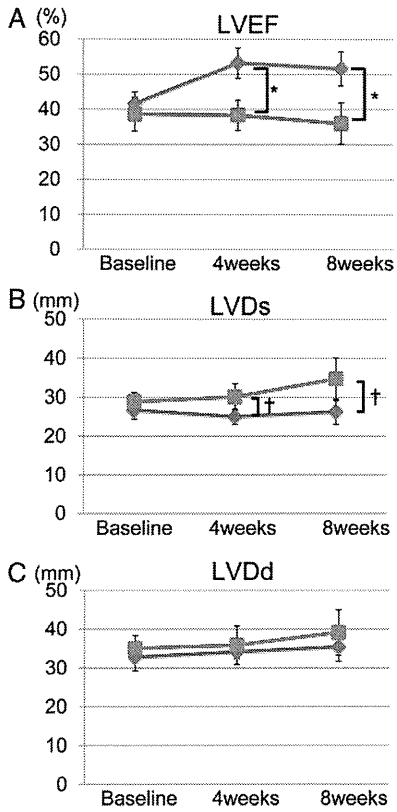

Figure 3. Echocardiographic evaluation. **A**, The global cardiac function as assessed by left ventricular ejection fraction (LVEF) was significantly better in the iPS group. **B**, The left ventricular end-systolic diameter (LVDs) was significantly smaller in the iPS group than in the sham group. **C**, The left ventricular end-diastolic diameter (LVDd) did not differ significantly between the iPS and sham groups. *$P<0.01$, †$P<0.05$ versus sham. The red line indicates the iPS group and the blue line the sham group. iPS indicates induced pluripotent stem cells.

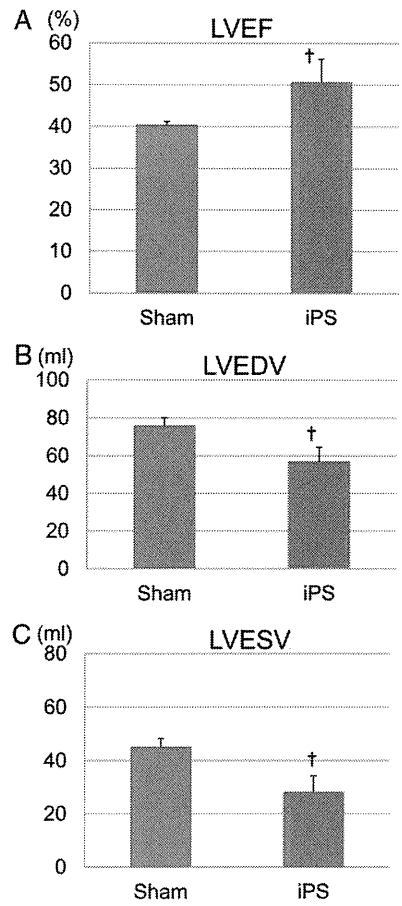

Figure 4. Cardiac multislice CT analysis. **A**, The global cardiac function as assessed by LVEF was significantly better in the iPS group. **B–C**, The left ventricular end-diastolic (LVEDV; **B**) and end-systolic (LVESV; **C**) volumes were significantly smaller in the iPS group than in the sham group. †$P<0.05$ versus sham. LVEF indicates left ventricular ejection fraction; iPS, induced pluripotent stem cells.

ization were quantified by real-time polymerase chain reaction 8 weeks after the treatment. The expression levels of vascular endothelial growth factor and basic fibroblast growth factor in the border area were significantly greater in the iPS group than in the sham group (Figure 7).

Phenotypic Fate of the Transplanted iPS-CMs in the Heart

The hiPS-CMs were labeled in vitro with a red fluorescent marker before transplantation. The labeled cells were identified on the surface of the heart 2 weeks after transplantation. Some of these cells were positive for slow myosin heavy chain (Figure 8A–D). Because the labeled cells could no longer be identified by 8 weeks after transplantation, the presence of the transplanted cells was assessed by fluorescence in situ hybridization using a human-specific genomic probe 8 weeks after transplantation. A small number of human genome-positive cells that expressed slow myosin heavy chain remained present in the infarct area (Figure 8E–G).

Discussion

The major findings of this study were as follows: (1) the newly developed culture system for hiPS cells successfully yielded approximately 2.5×10^7 highly pure hiPS-CMs, and hiPS-CM sheets could be made from these high pure hiPS-CMs using temperature-responsive dishes; (2) the hiPS-CM sheets survived in damaged myocardium in the short term and improved cardiac function in a porcine ischemic cardiomyopathy model, chiefly through the paracrine effects of cytokines. Histological analysis indicated that transplantation of hiPS sheets attenuated left ventricular remodeling and increased neovascularization; and (3) hiPS-derived cardiomyocytes could still be detected 8 weeks after transplantation, but the number of hiPS-CMs that survived long term was very small. No teratoma formation was observed in animals that received hiPS-CM sheets.

The optimal number of cells for clinical use of cardiac regeneration therapy remains unknown. Implantation of approximately 10^8 to 10^9 cells was shown to produce cardiac improvement in previous clinical trials using bone marrow-derived cells.[16] Given these results, it may be necessary to transplant almost this number of hiPS-CMs into impaired myocardium to improve cardiac function in a clinical setting. It is challenging to obtain large numbers of hiPS-CMs at high purity because clinical application of hiPS cells requires 3 steps (ie, proliferation, differentiation, and purification). In

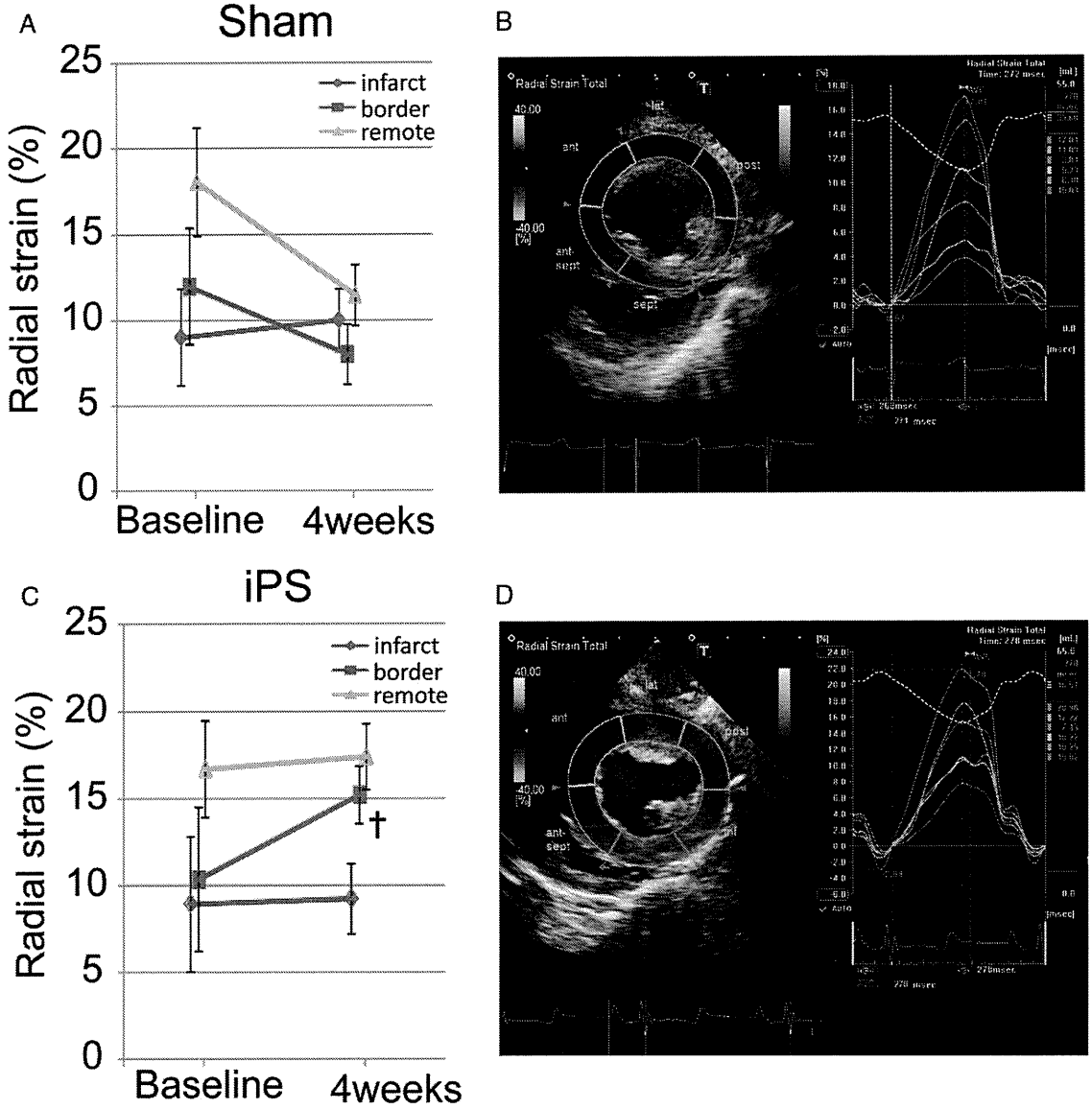

Figure 5. Evaluation of regional wall motion by 2-dimensional speckle-tracking echocardiography. Representative examples of radial strain analysis in each group are shown in **B** (sham) and **D** (iPS). **A**, In the sham group, the radial strain values of all areas did not differ significantly between the baseline and 4 weeks after the sham operation. **C**, In the iPS group, the radial strain value of the border area of the infarct was significantly greater 4 weeks after treatment than at baseline. The radial strain values of the other areas relative to the infarct did not differ significantly before and after hiPS-CM-sheet transplantation. †$P<0.05$ versus baseline. iPS indicates induced pluripotent stem cells; hiPS-CM, human induced pluripotent stem cell-derived cardiomyocyte.

the present study, we obtained approximately 2.5×10^7 hiPS-CMs after differentiation and purification of hiPS cells. One advantage of our culture system for hiPS cells its simplicity, because it involves only supplementation with cytokines for differentiation and culture in glucose-free medium for purification. Our culture system might be able to yield higher numbers of hiPS-CMs and could, possibly, be expanded to a clinically useful scale. Moreover, a previous study evaluating the propensity of secondary neurospheres generated from iPS cells to form teratomas found a significant correlation between the teratoma diameter and the proportion of undifferentiated cells in the secondary neurospheres.[17] Importantly, no teratoma formation was detected in the current experiment, which could be because our purification method limited the number of undifferentiated iPS cells in the hiPS-CMs.

Structural connection and electromechanical integration have been considered to be the mechanisms of functional recovery of the impaired myocardium after ES cell-derived cardiomyocyte transplantation.[18,19] We therefore predicted that the hiPS-CMs would connect structurally and electromechanically with the host myocardium, as seen for ES cell-derived cardiomyocytes. However, although functional cardiac recovery was observed after hiPS-CM-sheet transplantation, only a few transplanted cells were persistently present. It has been shown that the therapeutic effects of stem cell therapy can result from paracrine or direct effects. Paracrine effects have been considered as the major mechanisms responsible for the therapeutic efficacy of cell therapy with somatic tissue-derived stem or progenitor cells. These effects classically refer to the ability of transplanted cells to extracellularly

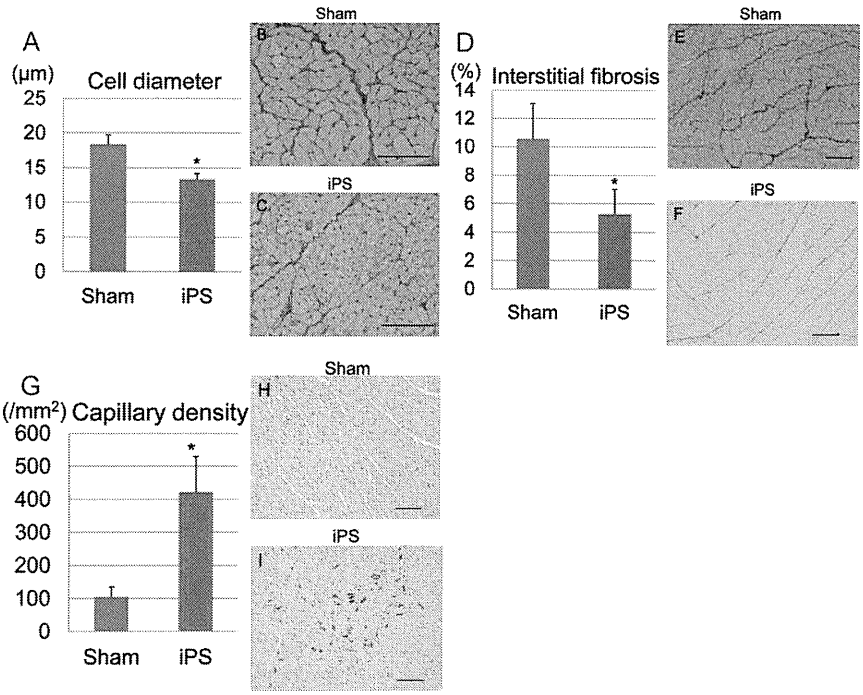

Figure 6. Histological evaluation after hiPS-CM-sheet transplantation. **A–C**, The diameters of the cardiomyocytes were measured at an area remote from the infarct; cardiomyocyte hypertrophy was significantly lower in the iPS group than in the sham group (**A**). Photomicrographs of periodic acid-Schiff (PAS)-stained sections are shown in **B–C**. **D–F**, The proportions of fibrosis-occupied area (%) at a site remote from the infarct; Picrosirius red staining demonstrated significantly less interstitial fibrosis in the iPS group than in the sham group (**D**). Photomicrographs of the Picrosirius red-stained sections are shown in **E–F**. **G–I**, Capillary density in an area bordering the infarct; the capillary density as assessed by immunostaining with an anti-von Willebrand factor antibody was significantly better in the iPS group (**G**). Photomicrographs of immunostaining for von Willebrand factor are shown in **H–I**. *$P<0.01$ versus sham. Bar=100 μm. hiPS-CM indicates human induced pluripotent stem cell-derived cardiomyocyte; iPS, induced pluripotent stem cells.

release various cardioprotective factors into the damaged cardiac tissue to directly enhance reverse LV remodeling. In contrast, recent reports have suggested that cell transplantation upregulates various cardioprotective factors native to the cardiac tissue through "crosstalk" between the transplanted cells and the native cardiac tissue.[2,20] In addition, another report has shown that paracrine effects of human cardiosphere-derived cells, which are capable of directed cardiac regeneration in vivo, play important roles in improving infarcted myocardium.[21] In our study, we observed that several factors, which were reportedly involved in cardiac repair,[20] were secreted by hiPS-CMs during in vitro screening. Consequently, cardiomyocyte hypertrophy and interstitial fibrosis were significantly attenuated in the infarct-remote area after cell sheet transplantation. In addition, capillary density was increased in the infarct border area associated with the upregulation of vascular endothelial growth factor and basic fibroblast growth factor after cell sheet transplantation. Speckle-tracking echocardiography showed that the regional function in the corresponding area was preserved after cell sheet transplantation as compared with that after a sham operation, in which the regional function progressively deteriorated. This suggests that ischemia-related hibernation in the infarct border myocardium might have recovered by increased blood flow because of angiogenesis. These findings suggest that in our study, paracrine effects are the major mechanisms underlying the functional improvement after hiPS-CM-sheet implantation. In contrast, only a small fraction of the transplanted cells differentiated into cardiac lineage, as assessed by fluorescence in situ hybridization analysis, which clearly distinguished cells of human origin from porcine cardiac tissue. This finding suggests that direct effects were not a major contributing mechanism responsible for the functional benefits observed in this study. Therefore,

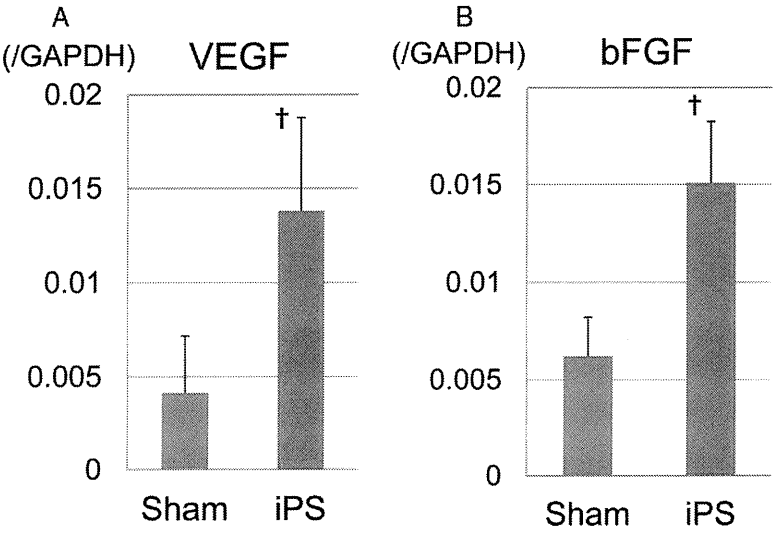

Figure 7. Neovascularization-related mRNA expression in an area bordering the infarct measured by real-time polymerase chain reaction (RT-PCR). The mRNA expression levels of vascular endothelial growth factor (VEGF; **A**) and basic fibroblast growth factor (bFGF; **B**) were significantly higher in the iPS group than in the sham group. †$P<0.05$ versus sham. iPS indicates induced pluripotent stem cells.

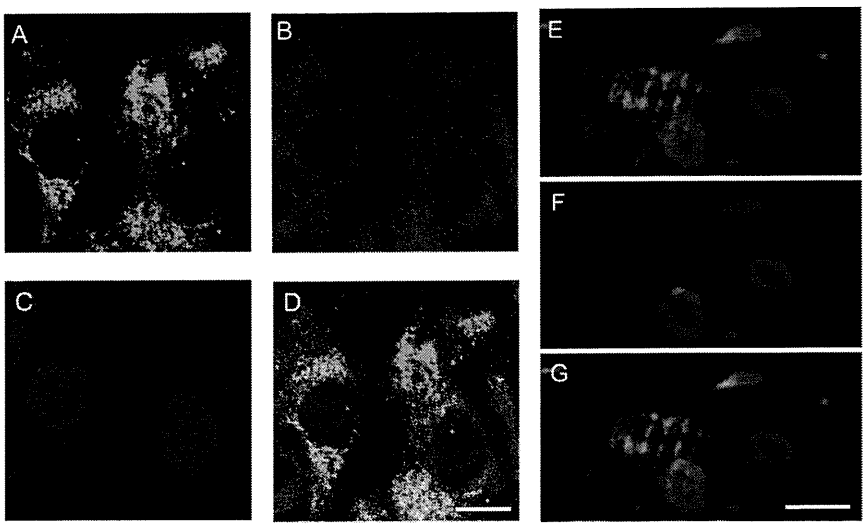

Figure 8. The hiPS-CMs in the heart after transplantation. **A–D**, Detection of red fluorescence-labeled hiPS-CMs 2 weeks after transplantation; representative photomicrographs showing slow myosin heavy chain (sMHC) in green (**A**) and labeled hiPS-CMs in red (**B**). **E–G**, Detection of hiPS-CMs 8 weeks after transplantation by fluorescence in situ hybridization (FISH) using a human-specific genomic probe; immunostaining for sMHC is shown in green (**E**) and positive FISH signals in red (**F**). The nuclei were stained with DAPI in blue (**C, E, F**). Merged images are shown in **D** and **G**. Bar=10 μm in **D** and **G**. hiPS-CM indicates human induced pluripotent stem cell-derived cardiomyocyte; DAPI, 4′,6-diamidino-2-phenylindole dihydrochloride.

it will be important to develop additive treatment to enhance survival, differentiation, and integration of the transplanted cells into the cardiac tissue.

Histological analysis revealed that most of the implanted hiPS-CMs disappeared after implantation, indicating poor engraftment of the hiPS-CMs into the impaired myocardium. In our study, hiPS-CMs secreted multiple angiogenic factors or their inducers, and the hiPS-CMs included small populations of CD31- or CD34-positive cells. These findings indicate that the hiPS-CM sheets have angiogenic potential, which might result in the generation of new vascular networks between the hiPS-CM sheets and the host cardiac tissue. A previous report has shown that the prompt formation of a vascular network between the cell sheet and the surrounding host tissue can sufficiently supply blood and oxygen to the transplanted cell sheet to survive and function in the host tissue.[22] However, in the present study, the host myocardium persistently experienced low blood supply due to coronary artery occlusion, which can interfere with the formation of a new vascular network between the cardiac tissue and the transplanted hiPS-CM sheets, possibly leading to poor survival and differentiation of the transplanted cells in the heart. Poor engraftment has been shown after experimental transplantation of human ES cell-derived cardiomyocytes through simple injection into the infarcted myocardium; treatment with several factors that block cell death pathways improved the engraftment of transplanted ES cell-derived cardiomyocytes.[23] We recently established a new method of cell protection by gene transfection[24] and a novel cell delivery system using the omentum,[25] which can enhance the therapeutic effects of cell therapy. Additional methods of prolonging cell survival after implantation might be necessary to improve the engraftment rate and thus obtain long-standing therapeutic effects of the hiPS-CM sheet from not only paracrine factors, but also direct contributions to the host heart.

Successful regeneration therapy using human pluripotent stem cells requires that the stem cells or their derivatives remain in the recipient myocardium long term. Unless the cell transplantation is autogeneic, the cells will inevitably be rejected by the immune system. Future clinical applications of hiPS cells for regeneration therapy may involve allogeneic and HLA type-matched transplantations, because some acute injuries such as myocardial infarction, stroke, or spinal cord trauma are targeted for regeneration therapy.[26] Therefore, elimination of immunologic rejection or induction of immunologic tolerance of the transplanted stem cells or their derivatives is a critical issue in stem cell-based medicine.[27] In the present study, we used tacrolimus as the only immunosuppressant in a xenotransplantation model; therefore, the failure of prolonged engraftment of hiPS-CMs could have been due to insufficient immunosuppressive therapy. A previous study has demonstrated that combined therapy with tacrolimus and sirolimus significantly prolonged the survival of human ES cells in a xenotransplantation model.[28] In another experiment, blocking the leukocyte costimulatory molecules was found to promote successful engraftment of ES and iPS cells in allogeneic and xenogeneic transplantation models.[26] These findings indicate that appropriate immunosuppressive therapies could improve stem cell engraftment. However, the immunogenicity of iPS cells has not yet been fully investigated. Further studies are needed to establish appropriate strategies for inducing and maintaining immunologic tolerance during the clinical use of allogeneic iPS cell therapy.

In conclusion, the present study showed that our culture system yields a large number of highly pure hiPS-CMs and that hiPS-CM sheets could improve cardiac function in the context of ischemic cardiomyopathy, primarily through paracrine cytokine effects. This newly developed culture system and the hiPS-CM sheets may provide a basis for clinical hiPS-CM-sheet transplantation as part of a strategy for promoting the regeneration of damaged myocardium.

Acknowledgments

We thank Shigeru Matsumi, Masako Yokoyama, and Akima Harada for excellent technical assistance.

Disclosures

Dr Shimizu is a consultant for CellSeed, Inc. Dr Okano is an Advisory Board Member in CellSeed, Inc, and an inventor/developer designated on the patent for temperature-responsive culture surfaces.

References

1. Jessup M, Brozena S. Heart failure. *N Engl J Med.* 2003;348:2007–2018.
2. Gonzales C, Pedrazzini T. Progenitor cell therapy for heart disease. *Exp Cell Res.* 2009;315:3077–3085.
3. Takahashi K, Yamanaka S. Induction of pluripotent stem cells from mouse embryonic and adult fibroblast cultures by defined factors. *Cell.* 2006;126:663–676.
4. Takahashi K, Tanabe K, Ohnuki M, Narita M, Ichisaka T, Tomoda K, Yamanaka S. Induction of pluripotent stem cells from adult human fibroblasts by defined factors. *Cell.* 2007;131:861–872.
5. Yu J, Vodyanik MA, Smuga-Otto K, Antosiewicz-Bourget J, Frane JL, Tian S, Nie J, Jonsdottir GA, Ruotti V, Stewart R, Slukvin II, Thomson JA. Induced pluripotent stem cell lines derived from human somatic cells. *Science.* 2007;318:1917–1920.
6. Germanguz I, Sedan O, Zeevi-Levin N, Shtrichman R, Barak E, Ziskind A, Eliyahu S, Meiry G, Amit M, Itskovitz-Eldor J, Binah O. Molecular characterization and functional properties of cardiomyocytes derived from human inducible pluripotent stem cells. *J Cell Mol Med.* 2011;15:38–51.
7. Ren Y, Lee MY, Schliffke S, Paavola J, Amos PJ, Ge X, Ye M, Zhu S, Senyei G, Lum L, Ehrlich BE, Qyang Y. Small molecule Wnt inhibitors enhance the efficiency of BMP-4-directed cardiac differentiation of human pluripotent stem cells. *J Mol Cell Cardiol.* 2011;51:280–287.
8. Yamashita JK. ES and iPS cell research for cardiovascular regeneration. *Exp Cell Res.* 2010;316:2555–2559.
9. Yoshida Y, Yamanaka S. iPS cells: a source of cardiac regeneration. *J Mol Cell Cardiol.* 2011;50:327–332.
10. Masuda S, Shimizu T, Yamato M, Okano T. Cell sheet engineering for heart tissue repair. *Adv Drug Deliv Rev.* 2008;60:277–285.
11. Memon IA, Sawa Y, Fukushima N, Matsumiya G, Miyagawa S, Taketani S, Sakakida SK, Kondoh H, Aleshin AN, Shimizu T, Okano T, Matsuda H. Repair of impaired myocardium by means of implantation of engineered autologous myoblast sheets. *J Thorac Cardiovasc Surg.* 2009;130:646–653.
12. Miyagawa S, Saito A, Sakaguchi T, Yoshikawa Y, Yamauchi T, Imanishi Y, Kawaguchi N, Teramoto N, Matsuura N, Iida H, Shimizu T, Okano T, Sawa Y. Impaired myocardium regeneration with skeletal cell sheets. A preclinical trial for tissue-engineered regeneration therapy. *Transplantation.* 2010;90:364–372.
13. Jaroszeski MJ, Gilbert R, Heller R. Detection and quantitation of cell–cell electrofusion products by flow cytometry. *Anal Biochem.* 1994;216:271–275.
14. Teramoto N, Koshino K, Yokoyama I, Miyagawa S, Zeniya T, Hirano Y, Fukuda H, Enmi J, Sawa Y, Knuuti J, Iida H. Experimental pig model of old myocardial infarction with long survival leading to chronic left ventricular dysfunction and remodeling as evaluated by PET. *J Nucl Med.* 2011;52:761–768.
15. Teichholz LE, Kreulen T, Herman MV, Gorlin R. Problems in echocardiographic volume determinations: echocardiographic–angiographic correlations in the presence or absence of asynergy. *Am J Cardiol.* 1976;37:7–11.
16. Rosenzweig A. Cardiac cell therapy—mixed results from mixed cells. *N Engl J Med.* 2006;355:1274–1277.
17. Miura K, Okada Y, Aoi T, Okada A, Takahashi K, Okita K, Nakagawa M, Koyanagi M, Tanabe K, Ohnuki M, Ogawa D, Ikeda E, Okano H, Yamanaka S. Variation in the safety of induced pluripotent stem cell lines. *Nat Biotechnol.* 2009;27:743–745.
18. Caspi O, Huber I, Kehat I, Habib M, Arbel G, Gepstein A, Yankelson L, Aronson D, Beyar R, Gepstein L. Transplantation of human embryonic stem cell-derived cardiomyocytes improves myocardial performance in infarcted rat hearts. *J Am Coll Cardiol.* 2007;50:1884–1893.
19. Kehat I, Khimovich L, Caspi O, Gepstein A, Shofti R, Arbel G, Huber I, Satin J, Itskovitz-Eldor J, Gepstein L. Electromechanical integration of cardiomyocytes derived from human embryonic stem cells. *Nat Biotechnol.* 2004;22:1282–1289.
20. Gnecchi M, Zhang Z, Ni A, Dzau VJ. Paracrine mechanisms in adult stem cell signaling and therapy. *Circ Res.* 2008;103:1204–1219.
21. Chimenti I, Smith RR, Li TS, Gerstenblith G, Messina E, Giacomello A, Marbán E. Relative roles of direct regeneration versus paracrine effects of human cardiosphere-derived cells transplanted into infarcted mice. *Circ Res.* 2010;106:971–980.
22. Shimizu T, Sekine H, Yang J, Isoi Y, Yamato M, Kikuchi A, Kobayashi E, Okano T. Polysurgery of cell sheet grafts overcomes diffusion limits to produce thick, vascularized myocardial tissues. *FASEB J.* 2006;20:708–710.
23. Laflamme MA, Chen KY, Naumova AV, Muskheli V, Fugate JA, Dupras SK, Reinecke H, Xu C, Hassanipour M, Police S, O'Sullivan C, Collins L, Chen Y, Minami E, Gill EA, Ueno S, Yuan C, Gold J, Murry CE. Cardiomyocytes derived from human embryonic stem cells in pro-survival factors enhance function of infarcted rat hearts. *Nat Biotechnol.* 2007;25:1015–1024.
24. Miyagawa S, Sawa Y, Taketani S, Kawaguchi N, Nakamura T, Matsuura N, Matsuda H. Myocardial regeneration therapy for heart failure: hepatocyte growth factor enhances the effect of cellular cardiomyoplasty. *Circulation.* 2002;105:2556–2561.
25. Shudo Y, Miyagawa S, Fukushima S, Saito A, Shimizu T, Okano T, Sawa Y. Novel regenerative therapy using cell-sheet covered with omentum flap delivers a huge number of cells in a porcine myocardial infarction model. *J Thorac Cardiovasc Surg.* 2011;142:1188–1196.
26. Pearl JI, Lee AS, Leveson-Gower DB, Sun N, Ghosh Z, Lan F, Ransohoff J, Negrin RS, Davis MM, Wu JC. Short-term immunosuppression promotes engraftment of embryonic and induced pluripotent stem cells. *Cell Stem Cell.* 2011;8:309–317.
27. Chidgey AP, Layton D, Trounson A, Boyd RL. Tolerance strategies for stem-cell-based therapies. *Nature.* 2008;453:330–337.
28. Swijnenburg RJ, Schrepfer S, Govaert JA, Cao F, Ransohoff K, Sheikh AY, Haddad M, Connolly AJ, Davis MM, Robbins RC, Wu JC. Immunosuppressive therapy mitigates immunological rejection of human embryonic stem cell xenografts. *Proc Natl Acad Sci U S A.* 2008;105:12991–12996.

Supplemental Materials

MS ID#: CIRCULATIONAHA/2011/084343

Feasibility, Safety, and Therapeutic Efficacy of Human Induced Pluripotent Stem Cell-derived Cardiomyocyte Sheets in a Porcine Ischemic Cardiomyopathy Model

Materials and Methods

All experimental procedures were approved by the institutional ethics committee. Animal care was conducted humanely in compliance with the "Principles of Laboratory Animal Care" formulated by the National Society for Medical Research and the "Guide for the Care and Use of Laboratory Animals" prepared by the Institute of Animal Resources and published by the National Institutes of Health (Publication No 85-23, revised 1996).

Culture, differentiation, and purification of human iPS cells and collection of conditioned medium

The human iPS (hiPS) cell line 201B7 that was generated using the 4 transcription factors Oct4, Sox2, Klf4, and c-Myc (a generous gift from Professor Yamanaka, Kyoto University, Japan) was used in this study[1]. The hiPS cells were cultured on matrigel™ (BD Bioscience, San Jose, CA)-coated dishes in mTeSR1 medium (Stem Cell Technologies, Vancouver, BC, Canada) that was changed daily. Human iPS cells were then dissociated using StemPro® Accutase® Cell

Dissociation Reagent (Invitrogen, Carlsbad, CA), transferred to Corning® ultra-low-attachment surface culture dishes (Sigma-Aldrich Corp., St. Louis, MO) at a density of 50,000 cells/mL in mTeSR1 with Y-27632 (Wako Pure Chemical Industries, Osaka, Japan), and cultured for 4 days to allow them to form embryoid bodies (EBs). The EBs were re-plated with differentiation medium (DM; DMEM-F12, Invitrogen) containing 20% fetal bovine serum (FBS), 100 μM nonessential amino acids (Invitrogen), 50 U/mL penicillin, 50 mg/mL streptomycin (Invitrogen), and 5.5 mM 2-mercaptoethanol (Invitrogen) and supplemented with 100 ng/mL Wnt3a (R&D Systems, Minneapolis, MN) and 100 ng/mL R-Spondin-1 (Stem RD, Burlingame, CA) and cultured for 2 days. The culture medium was then replaced with DM without the supplemental factors for 2 days and then changed to DM supplemented with 100 ng/mL Dkk1 (R&D Systems) for 2 days. On day 10, the EBs were plated on gelatin-coated dishes in DM, which was refreshed every 2 days.

The culture medium was subsequently replaced with glucose-free DMEM (Invitrogen) with 1 mM lactic acid (Wako) (Hattori, F. and Fukuda, K. WO2007/088874; PCT/JP2007/051563, 2007) on day 20 and changed to DMEM/10% FBS the next day. On day 25, the culture medium was again replaced with glucose-free DMEM with 1 mM lactic acid and changed to DMEM/10% FBS the next day; this procedure eventually generated pure hiPS cell-derived cardiomyocytes (hiPS-CM). The hiPS-CMs were then labeled with a red fluorescent marker (CellTracker Red CMTPX, Invitrogen), as previously described[2]. FBS-free DMEM media were conditioned by hiPS-CMs for 48 hours after the completion of our differentiation and purification protocols. A total

of 48 cytokines and growth factors were measured by the Bio-Plex human cytokine assay (Bio-Rad, UK) for *in-vitro* screening.

Preparation of hiPS cell-derived cardiomyocyte sheets

The hiPS-CMs were detached using StemPro® Accutase® Cell Dissociation Reagent and seeded onto 6-cm UpCell dishes (CellSeed, Tokyo, Japan) at a density of 4×10^6 cells/dish in combination with normal human dermal fibroblasts (NHDF; Lonza, Basel, Switzerland) at 8×10^5 cells/dish. The next day, the dish was incubated at room temperature, which caused the cells to detach spontaneously to form a scaffold-free hiPS-CMs sheet.

Generation of the porcine chronic myocardial infarction model

Twelve female mini-pigs (Japan Farm, Kagoshima, Japan) weighing 20 to 25 kg were pre-anesthetized with ketamine hydrochloride (20 mg/kg, DAIICHI SANKYO, Tokyo, Japan) and xylazine (2 mg/kg, Bayer HealthCare, Leverkusen, Germany), intubated endotracheally (6 Fr Sheridan, InterMed Japan, Osaka, Japan), and maintained under general anesthesia by a continuous infusion of propofol (6 mg/kg/h, Astra-Zeneca) and vecuronium bromide (0.05 mg/kg/h), DAIICHI SANKYO). The pericardial space was exposed by left thoracotomy through the fourth intercostal space. The distal portion of the left anterior descending coronary artery (LAD) was ligated directly, and an ameroid constrictor (COR-2.50-SS, Research Instruments) was placed

around the LAD just distal to the branch point of the left circumflex coronary artery[3]. The muscle and skin were closed in layers, and the mini-pigs were then allowed to recover and maintained in temperature-controlled individual cages for 4 weeks.

Transplantation of hiPS-CMs sheets

All animals were immunosuppressed by daily administration of tacrolimus (0.6 mg/kg, Astellas, Tokyo, Japan) from 5 days before transplantation until sacrifice. Four weeks after the ameroid placement, the mini-pigs were randomly divided into 2 treatment groups (n = 6 each) to undergo either hiPS-CMs sheet transplantation (iPS group) or sham operation.

The hiPS-CMs sheets were transplanted via median sternotomy under general anesthesia. The area of the myocardial infarct was identified visually on the basis of surface scarring and abnormal wall motion. In the iPS group, 8 hiPS-CM sheets were transplanted over the infarcted myocardium. Two layers of hiPS-CM sheets were stacked over the broad surface of the myocardium. The mini-pigs were then allowed to recover in temperature-controlled individual cages and were later humanely sacrificed for analysis. The excised heart and other thoracic organs were visually inspected for possible tumor formation.

Standard and 2D speckle-tracking echocardiography

Transthoracic echocardiography was performed under general anesthesia using a 5.0-MHz transducer (Aplio Artida; Toshiba, Otawara, Japan). The left ventricular (LV) end-diastolic and end-systolic diameters (LVDd and LVDs, respectively) were measured in M-mode in the short-axis view, while the LV end-diastolic and end-systolic volumes (LVEDV and LVESV, respectively) were calculated from the Teichholz formula[4]. The LV ejection fraction (LVEF) was calculated from the following formula: LVEF (%) = 100 × (LVEDV - LVESV)/(LVEDV). The data are presented as the average of the measurements over 3 continuous beats.

Two-dimensional speckle-tracking echocardiography (2DSE) analysis was performed using the customized 2DSE software for the Toshiba system (2D Wall Motion Tracking, Toshiba Medical Systems). The endocardial border was traced manually, and a region of interest was drawn to include the entire myocardium. The software algorithms automatically segmented the LV planes into equidistant segments and performed speckle tracking on a frame-to-frame basis. The studies were assessed visually, and abnormal curves that appeared to be artifactual were excluded. Regional cardiac function was evaluated using radial strain values obtained from the mid-short-axis plane. The anterior and anteroseptal segments were defined as the infarct area, while the lateral and inferoseptal segments were defined as the border area and the posterior and inferior segments as the remote area. The strain value of each area was calculated from the average of 2 segments and expressed as a percentage (%).

Cardiac computed tomography scan

Electrocardiogram-gated multislice computed tomography (MSCT) was performed under general anesthesia in the supine position during end-expiratory breathhold with a 16-slice MSCT scanner (Somatron Emotion 16, Siemens, Forchheim, Germany). A standardized examination protocol was applied using 16 × 0.75-mm collimation, a 3.4-mm table feed per rotation, and a tube rotation time of 420 ms. The tube voltage was 120 kV with 500 effective mAs. MSCT was performed after intravenous injection of 90 mL of non-ionic contrast medium (Iomeprol, Bracco Imaging, Konstanz, Germany). Axial images were reconstructed using the scanner software. All images were analyzed on a workstation (AZE, Virtual Place Lexus 64). LVEDV and LVESV were obtained from the workstation and LVEF was calculated using the formula described above.

Holter electrocardiogram

Holter electrocardiogram (ECG) was performed for 24 hours in both groups (n = 6 each). The arrhythmogenesis associated with hiPS-CMs sheet transplantation was evaluated based on the number of premature ventricular contractions.

Histology and immunohistolabeling

Dissociated cultured cells were fixed in 4% paraformaldehyde for 20 minutes at room temperature, washed 3 times with phosphate-buffered saline (PBS), permeabilized with 0.2% Triton X-100 for

30 minutes, and blocked with 3% BSA in PBS for 2 hours. The primary antibodies used included anti-cardiac troponin T (cTNT, 1:100 dilution, Abcam, Cambridge, UK), anti-Nkx2.5 (1:100 dilution, Santa Cruz Biotechnology, Santa Cruz, CA), anti-α-actinin (1:100 dilution, Sigma-Aldrich Corp.), anti-human CD31 (1:100 dilution, BD Biosciences, San Jose, CA), anti-human CD34 (1:100 dilution, BD Biosciences), and anti-vimentin (1:100 dilution, BD Biosciences) and were visualized by fluorophore-conjugated secondary antibodies such as AlexaFluor488 goat anti-rabbit IgG, AlexaFluor488 goat anti-mouse IgG, and AlexaFluor488 donkey anti-goat IgG (1:1000 dilution, Invitrogen) with counterstaining by 4′,6-diamidino-2-phenylindole (DAPI, Dojindo, Tokyo, Japan) and assessed by fluorescence microscopy. Images of the samples were acquired with a Biorevo BZ-9000 (Keyence, Osaka, Japan). Positivity of the cardiomyocyte-specific markers or other lineage markers in the cultured cells was determined from the acquired images by using computer-based cell counting with the Dynamic Cell Count BZ-H1CE software (Keyence).

The excised heart specimens were either fixed with 10% buffered formalin and embedded in paraffin or fixed with 4% paraformaldehyde, embedded in OCT compound (Tissue Tek; Sakura Finetek, Torrance, CA), and snap-frozen. The paraffin-embedded sections were stained with Picrosirius red or periodic acid-Schiff (PAS) to assess interstitial fibrosis and cardiomyocyte hypertrophy, respectively[5,6]. The paraffin-embedded sections were immunolabeled with anti-human von Willebrand factor antibody (Dako, Glostrup, Denmark) and visualized with the horseradish peroxidase-based EnVision kit (Dako) according to the manufacturer's instructions.